Eur Biophys J (2003) 32: 671–675
DOI 10.1007/s00249-003-0331-x

ARTICLE

David G. Regan · Philip W. Kuchel

# Simulations of NMR-detected diffusion in suspensions of red cells: the effects of variation in membrane permeability and observation time

Received: 6 March 2003 / Revised: 13 May 2003 / Accepted: 13 May 2003 / Published online: 12 July 2003


**Abstract** Monte Carlo random-walk simulations of diffusion in virtual lattices of cells have been used to study and characterize diffusion-coherence phenomena that arise when pulsed field-gradient spin-echo (PGSE) nuclear magnetic resonance (NMR) experiments are conducted on human red blood cell (RBC; erythrocytes) suspensions. These coherence effects are manifest as diffraction-like patterns when the normalized PGSE signal intensities are plotted as a function of the spatial wave vector **q** in so-called *q*-space plots. **q**-Space analysis is sensitive to small changes in cell morphology, cell size, membrane transport rates, hematocrit, and packing arrangement. In the present study we used simulations to predict the effect of varying the time over which diffusion is measured (the ''observation time'' or ''diffusion time'') and the permeability of the membrane on the form of **q**-space plots. Thus we predict that inhibiting water exchange across the human RBC membrane, such that the value of the permeability coefficient is reduced by approximately an order of magnitude below the normal physiological value, will effectively render the membrane impermeable on the timescale of the PGSE NMR experiment; further inhibition will therefore result in negligible reduction in the measured root-mean-square displacement (r.m.s.d.) of diffusing water as a function of the observation time. The work also underscores the importance of using an appropriate experimental observation time if **q**-space data are to be used to estimate compartment dimensions and interbarrier spacing, and illustrates an expeditious method for determining this value.

**Keywords** Erythrocyte · Membrane permeability · Monte Carlo · Pulsed field-gradient spin-echo

D. G. Regan (✉)
Graduate School of Biomedical Engineering,
University of New South Wales, NSW 2052, Australia
E-mail: d.regan@unsw.edu.au

P. W. Kuchel
School of Molecular and Microbial Biosciences,
University of Sydney, NSW 2006, Australia

## Introduction

Pulsed field-gradient spin-echo (PGSE) nuclear magnetic resonance (NMR) is now a well understood and accurate method for measuring molecular self-diffusion (Stilbs 1987; Kärger et al. 1988), even in heterogeneous samples (Kärger and Fleischer 1994). In the biological setting this technique is particularly useful for measuring molecular translational motion because it is non-invasive and, in contrast to many other techniques, does not require the establishment of a concentration gradient.

The PGSE NMR method is based on the encoding of spatial information in the phase of spin magnetization by the imposition of a magnetic field-gradient on the sample in order to measure positional displacement. In heterogeneous samples exhibiting a degree of local order, spatial coherences in the magnetization phase can result in diffraction- and interference-like effects which yield structural information at a spatial resolution that is inaccessible to conventional magnetic resonance imaging (Callaghan et al. 1991).

We have shown diffusion-coherence phenomena to be manifest in PGSE NMR diffusion data obtained from human red blood cell (RBC; erythrocytes) suspensions (Kuchel et al. 1997). When the normalized relative signal intensities from these experiments are plotted as a function of the spatial wave vector **q**, a pattern of maxima and minima is observed whose origin is mathematically analogous to that of optical single-slit diffraction and two-slit interference. These plots constitute profiles of the transport properties of the suspensions being investigated and yield information on cell dimensions, cell morphology, membrane permeability, and packing density (hematocrit; Ht) (Kuchel et al. 1997; Torres et al. 1998, 1999; Regan and Kuchel 2002).

In a recent paper published in this journal (Regan and Kuchel 2003), which will hereafter be referred to as Paper I, we used computer simulations to show that these profiles also contain ''signatures'', in the form of fine structures, that contain information regarding the

packing arrangement of the cells in the suspension. The present work, which is a continuation of this effort to characterize diffusion-coherence phenomena in cell suspensions, investigates the effects of varying experimental observation time and membrane permeability on the form of *q*-space plots. [In PGSE NMR methods for measuring molecular diffusion, the experimental observation time is the time interval separating the two radiofrequency pulses (Stilbs 1987; Kärger et al. 1988), Δ, and is sometimes referred to as the "diffusion time".]

## Methods

Monte Carlo simulations of diffusion of water in hexagonal lattices of biconcave disc-shaped cells were conducted for a range of observation times and for a range of membrane permeabilities. The methods used are described in detail in Paper I (Regan and Kuchel 2003). All simulations were conducted in the context of a PGSE NMR experiment and therefore yielded a set of signal intensities corresponding to the respective magnetic field-gradient strengths used. The values of simulation parameters were chosen according to their known values in real RBC suspensions and, in the case of PGSE NMR parameters, to be in accordance with those used in experiments on real RBC suspensions (Regan and Kuchel 2002, 2003).

Simulations were conducted with the observation time, Δ, set to the following values: 2, 3, 5, 10, 20, 40, and 100 ms. Simulations were also conducted with Δ fixed at 20 ms and with membrane permeability ($P_d$) set to the following values: 0, $6.1\times10^{-7}$, $6.1\times10^{-6}$, $6.1\times10^{-5}$ (the known permeability of real human RBC; Benga et al. 2000), and $6.1\times10^{-4}$ m $s^{-1}$. It should be noted that in the Monte Carlo random-walk model used here, and previously, to simulate diffusion in a cell suspension, the permeability coefficient of the membrane is related to the diffusion coefficient (*D*), the probability of transition across the membrane (*tp*) and the jump-size (*s*) by the following relationship (Regan and Kuchel 2000):

$$P_d = tpD/s \quad (1)$$

Root-mean-square displacements (r.m.s.d.) were calculated as the root of the mean of the squares of the overall displacements summed over all random walk trajectories in the simulation ($10^8$ trajectories per simulation).

## Results

### Varying the observation time

Simulations were conducted for diffusion of water in lattices of biconcave disc-shaped cells (whose dimensions and shape mimicked those of real human RBC) at observation times (Δ) of 2, 3, 5, 10, 20, 40, and 100 ms; the results are shown in Fig. 1. The r.m.s.d. values obtained from this series of simulations were 2.44, 2.79, 3.63, 4.67, 6.22, 8.54, and 13.22 μm, respectively; these results are illustrated in Fig. 2.

The *q*-space plots shown in Fig. 1 allow four key observations: (1) reduced signal intensity at given *q*-values as the observation time was increased; (2) absence of a discernible pore-hopping shoulder at the shortest observation times (Δ = 2, 3 ms) and an increase in prominence of this feature as the observation time was increased to higher values; (3) stabilization in the position of diffusion-diffraction peaks as the observation time was increased; and (4) the appearance of discernible fine structure (in the form of additional shoulders) in diffusion-diffraction peaks at the longest observation times (Δ = 20, 40, and 100 ms).

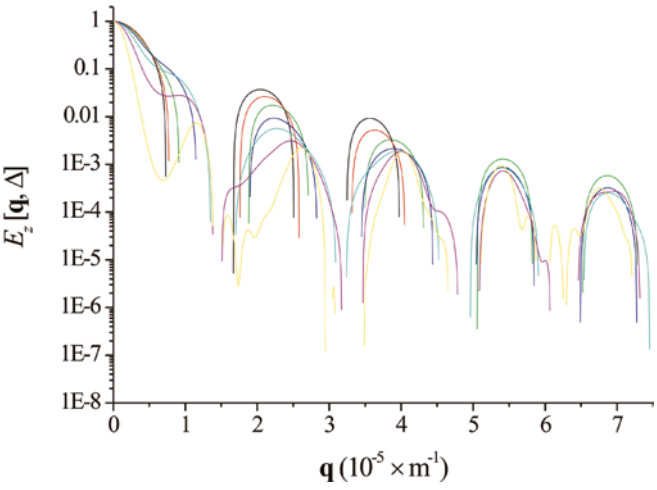


**Fig. 1** *q*-Space plots (normalized relative signal intensity, *E*, as a function of ***q***) for simulation of diffusion of water in a lattice of biconcave disc-shaped cells (of shape and dimensions that mimic those of human RBC) over a range of observation times (Δ). Key: *black*, Δ = 2 ms; *red*, Δ = 3 ms: *green*, Δ = 5 ms; *blue*, Δ = 10 ms; *cyan*, Δ = 20 ms; *magenta*, Δ = 40 ms; *yellow*, Δ = 100 ms

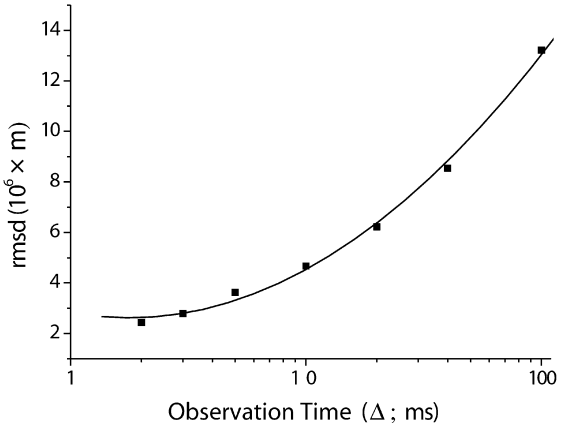


**Fig. 2** Root-mean-square displacements as a function of observation time (Δ; logarithmic scale). The curve fitted to the points in the graph is provided as a guide to the eye and is given by r.m.s.d. $= 10^{-6}(3.4\Delta^2 - 1.7\Delta + 2.8)$

### Varying the membrane permeability coefficient

Simulations were conducted for diffusion of water in lattices of cells (identical to those just described) in which Δ was fixed at 20 ms and membrane permeability was varied from the impermeable case ($P_d = 0$ m $s^{-1}$) to a maximum permeability of $6.1\times10^{-4}$ m $s^{-1}$; these results are shown in Fig. 3. The corresponding r.m.s.d. values measured from these simulations (ranging from lowest

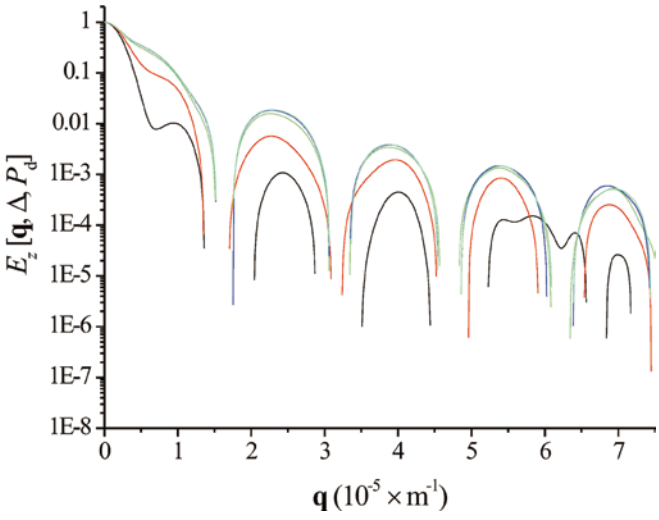


**Fig. 3** *q*-Space plots (normalized relative signal intensity,*E*, as a function of ***q***) for simulation of diffusion of water in a lattice of biconcave disc-shaped cells (of shape and dimensions that mimic those of human RBC) over a range of membrane permeabilities ($P_d$) with Δ fixed at 20 ms. Key: *black*, $P_d = 6.1\times10^{-4}$ m s$^{-1}$; *red*, $P_d = 6.1\times10^{-5}$ m s$^{-1}$; *green*, $P_d = 6.1\times10^{-6}$ m s$^{-1}$; *blue*, $P_d = 6.1\times10^{-7}$ m s$^{-1}$; *cyan*, $P_d = 0$ m s$^{-1}$

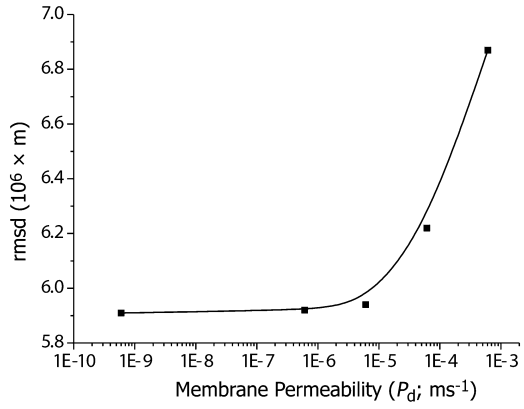


**Fig. 4** Root-mean-square displacements as a function of membrane permeability. Because the results are best illustrated on semi-logarithmic axes ($\log_{10}P_d$) such that the value at $P_d = 0$ m s$^{-1}$ could not ordinarily be displayed, we have plotted the value of the r.m.s.d. estimated for this permeability value at $P_d = 6.0\times10^{-10}$ m s$^{-1}$; this translates to a membrane transition probability in the order of $10^{-9}$ on the timescale of Δ and a permeability of zero for all practical purposes. The *line* connecting the points in the graph is provided as a guide to the eye and was achieved by applying a cubic B-spline to the data

to highest value of $P_d$) were 5.91, 5.92, 5.94, 6.22, and 6.87 μm, respectively; these results are graphed in Fig. 4. This figure shows that as the permeability was increased, the r.m.s.d. values increased in a highly nonlinear way.

Figure 3 allows the following four observations to be made: (1) reduced signal intensity at given *q*-values as the permeability was increased; (2) enhancement of the pore-hopping shoulder at the highest permeability values ($P_d = 6.1\times10^{-4}$and $6.1\times10^{-5}$ m s$^{-1}$) and more discernible fine structure in the diffusion-diffraction peaks at these values; (3) a second putative pore-hopping shoulder was discernible at the three lowest permeabilities; and (4) the curves for the two lowest permeabilities ($P_d = 6.1\times10^{-7}$and 0 m s$^{-1}$) were almost indistinguishable (out to at least$q = 4.5\times10^5$ m$^{-1}$).

## Discussion

Simulations of diffusion in lattices of biconcave disc-shaped cells were conducted to investigate the effects of altering diffusional observation time and membrane permeability on the form of the respective*q*-space plots. These two investigations were aimed at further characterizing *q*-space phenomena in cell suspensions. The first relates closely to the design of the PGSE NMR experiment that is used to measure cell dimensions and the second has implications for the detection of pathological states in cells and tissues.

### Varying the observation time

The general reduction in signal intensity, seen in Fig. 1, as the observation time was increased can be attributed directly to an increased r.m.s.d. The Einstein equation for unrestricted isotropic diffusion (Einstein 1956) indicates that the r.m.s.d. for a given diffusion coefficient (*D*) is proportional to the square root of the diffusional observation time. Therefore, a doubling of the observation time will result in an increase in the r.m.s.d. by a factor of √2. In the system discussed here, it cannot be assumed that this will be the case as the water is diffusing in two different compartments with different values of *D* and under different conditions of restriction (the extracellular water is considerably less restricted than the intracellular water). Indeed, an increase in Δ from 5 to 10 ms resulted in an increase in the r.m.s.d. by a factor of only 1.28. However, when Δ was increased from 10 to 20 ms, and from 20 to 40 ms, this factor rose to 1.33 and 1.37, respectively, reflecting the greater influence on this value of the faster and less restricted extracellular diffusion whose r.m.s.d. increases with increasing observation time. This trend is clearly illustrated in Fig. 2.

The increase in prominence of the pore-hopping shoulder (due to water diffusing between pores in the extracellular space) as Δ is increased, and the appearance of fine structure in the diffraction peaks at the longest values of Δ, are attributed to more extensive "mapping" of the extracellular cavities that results from longer observation times and consequently the greater degree, relative to free diffusion, to which the diffusion is restricted.

Perhaps the most important observation from this series of simulations was the shift of the diffraction peaks to higher *q*-values as Δ was increased, with this shift becoming less dramatic at the higher values of Δ. The extent of this shift is difficult to determine at the highest values of Δ owing to additional shoulders on these peaks which obscured their true maxima (the peaks

at $q \approx 5.5\times10^5$ and $7.5\times10^5$ m s$^{-1}$were less affected by this fine structure and their positions were virtually identical). The initial dramatic shift in position of these features, however, can be attributed to diffusion being less restricted at lower values of $\Delta$, with the r.m.s.d. consequently being time-dependent. By derivation from the Einstein equation for diffusion in one dimension, restricted diffusion can be said to occur when $\Delta \gg a^2/2D$, where $a$ is the mean dimension in the direction in which diffusion is being measured. In the simulations described here, where $a$ was approximately 6 $\mu$m, the positions of the diffraction peaks could therefore be expected to be dependent on $\Delta$ when its value fell below ~20 ms. This threshold value for $\Delta$ can be easily and more accurately determined, particularly if cell dimensions are not known, using the $q$-space method. Cell dimensions can then be estimated with greater certainty using this method by selecting a value of $\Delta$ which ensures that the measured diffusion lies in the restricted regime, where the positions of diffraction peaks, and the scaling factors that relate them to cell dimensions, are not dependent on the actual chosen value of $\Delta$.

### Varying the membrane permeability coefficient

The $q$-space plots for this series of simulations (Fig. 3) showed a general reduction in signal intensity as the membrane permeability was decreased. This result is attributable to the reduced measured r.m.s.d. for water in the system as the mean residence time of the intracellular component became longer. Clearly, at a fixed observation time, variations in$P_d$ will have far lesser effect on the mobility of the extracellular water. The enhancement of the pore-hopping shoulder at high permeabilities is due to a higher level of signal attenuation of the more mobile intracellular component of diffusion; at lower permeabilities there is less attenuation and the signal from the intracellular component tends to mask those features of the $q$-space plot which are due to the more rapidly diffusing extracellular component. We suggest that the additional putative pore-hopping shoulders discernible at the lowest permeabilities are due to water being more restricted and thereby revealing the topological features of the extracellular space which are not as well defined at higher permeabilities.

The observation that the $q$-space plots for the two lowest permeabilities are almost inseparable can be explained by reference to Fig. 4, which shows that at these permeabilities there is virtually no difference in the r.m.s.d. Interpretation of this figure suggests that, at $P_d$values below about $10^{-5}$ m s$^{-1}$ (when $\Delta = 20$ ms),[1] there will be negligible change in the r.m.s.d. values and that these will in fact be close to the r.m.s.d. observed when$P_d = 0$. Above this threshold value, the r.m.s.d. will increase steeply as the permeability is increased due to the increase in the rate of exchange of water between the intracellular and extracellular regions and consequently an increase in overall water mobility. This threshold permeability lies approximately one order of magnitude below the known normal permeability of $6.1\times10^{-5}$ m s$^{-1}$for human RBC (Benga et al. 2000). The implications of this finding are: (1) small changes in RBC membrane permeability from the normal value can be expected to result in large changes in water r.m.s.d.; and (2) a reduction in RBC membrane permeability of about one order of magnitude from the normal value is predicted to give rise to a reduction in the r.m.s.d. of water to a value close to that expected for an impermeable membrane, on the timescale of the NMR experiment. Assuming these results can be extrapolated to other cell types and, in particular, solid tissues, we suggest that the measurement of r.m.s.d. (as is indicated, for example, by the extent of signal attenuation in the $q$-space plot) may provide deeper insight than previously realized to pathological conditions in which transport properties are altered.

It has been predicted from an analytical study of diffusive transport through a spherical interface that diffusion-diffraction maxima and minima will move to higher $q$-values as the permeability increases (Barzykin et al. 1995). The present work does not support this proposal and we surmise that the explanation for this is that transport was bidirectional in this case, whereas the study mentioned only accounted for transport out of the spherical enclosure.

## Conclusions

The aim of the work was to provide additional insights to the measurement and analysis of diffusion-coherence phenomena in $q$-space plots from RBC suspensions. The two major conclusions of the present work are: (1) the $q$-positions of diffraction peaks depend on the observation time, specifically in the non-restricted diffusion regime; and (2) the highly nonlinear dependence of the measured or apparent r.m.s.d. on the permeability of the membrane. These findings have implications for the design of PGSE NMR experiments for the purpose of $q$-space analysis and for the application of $q$-space analysis in the clinical setting. This work further asserts the potential of $q$-space analysis for the non-invasive detection of changes in transport properties of cells and tissues due to pathological changes.

**Acknowledgements** The work was supported by a Project Grant to P.W.K. from the Australian Research Council. D.G.R. was supported by an Australian Postgraduate Award. Mr. Bill Lowe is thanked for general technical assistance. A/Prof. Russell Standish, Director of the High Performance Computing Support Unit at the University of New South Wales, is thanked for assistance in obtaining resource allocation on the APAC (Australasian Partnership for Advanced Computing) National Facility supercomputer, and in software implementation.

[1] This value will be dependent to some extent on $\Delta$ because at longer observation times the contribution to the r.m.s.d. of the extracellular component of diffusion will be greater

## References


Barzykin AV, Hayamizu K, Price WS, Tachiya M (1995) Pulsed-field-gradient NMR of diffusive transport through a spherical interface into an external medium containing a relaxation agent. J Magn Reson A 114:39–46

Benga G, Kuchel PW, Chapman BE, Cox GC, Ghiran I, Gallagher CH (2000) Comparative cell shape and diffusional water permeability of red blood cells from Indian elephant (*Elephas maximus*) and man (*Homo sapiens*). Comp Haematol Int 10: 1–8

Callaghan PT, Coy A, MacGowan D, Packer KJ, Zelaya FO (1991) Diffraction-like effects in NMR diffusion studies of fluids in porous solids. Nature 351:467–469

Einstein A (1956) Investigations on the theory of the Brownian movement. Dover, New York

Kärger J, Fleischer G (1994) NMR diffusion studies in heterogeneous systems. Trends Anal Chem 13:145–157

Kärger J, Pfeifer H, Heink W (1988) Principles and application of self-diffusion measurements by nuclear magnetic resonance. Adv Magn Reson 12:1–89

Kuchel PW, Coy A, Stilbs P (1997) NMR "diffusion-diffraction" of water revealing alignment of erythrocytes in a magnetic field and their dimensions and membrane transport characteristics. Magn Reson Med 37:637–643

Regan DG, Kuchel PW (2000) Mean residence time of molecules diffusing in a cell bounded by a semi-permeable membrane: Monte Carlo simulations and an expression relating membrane transition probability to permeability. Eur Biophys J 29:221–227

Regan DG, Kuchel PW (2002) Simulations of molecular diffusion in lattices of cells: insights for NMR of red blood cells. Biophys J 83:161–171

Regan DG, Kuchel PW (2003) Simulations of NMR-detected diffusion in suspensions of red cells: the "signatures" in *q*-space plots of various lattice arrangements. Eur Biophys J 31:563–574

Stilbs P (1987) Fourier transform pulsed-gradient spin-echo studies of molecular diffusion. Prog Nucl Magn Reson Spectrosc 19:1–45

Torres AM, Michniewicz RJ, Chapman BE, Young GAR, Kuchel PW (1998) Characterisation of erythrocyte shapes and sizes by NMR diffusion-diffraction of water: correlations with electron micrographs. Magn Reson Imaging 16:423–434

Torres AM, Taurins AT, Regan DG, Chapman BE, Kuchel PW (1999) Assignment of coherence features in NMR *q*-space plots to particular diffusion modes in erythrocyte suspensions. J Magn Reson 138:135–143